Proceedings of Australasian Conference on Robotics and Automation, 3-5 Dec 2012, Victoria University of Wellington, New Zealand.

Second-order Sliding Mode Control for Offshore Container Cranes

R. M. T. Raja Ismail and Q. P. Ha
Faculty of Engineering and Information Technology
University of Technology, Sydney, Australia
{Raja.RajaIsmail, Quang.Ha}@uts.edu.au

Abstract

Open-sea stevedores of containers provide an alternative way to avoid port congestion. This process involves a mobile harbour equipped with a crane which loads/unloads containers from a large cargo ship. However, the presence of ocean waves and gusty winds can produce an excessive sway to the hoisting ropes of the crane system. This paper presents a second-order sliding mode controller for trajectory tracking and sway suppression of an offshore container crane. From the proposed control law, the asymptotic stability of the closed-loop system is guaranteed in the Lyapunov sense. Simulation results indicate that the developed control system can achieve high performance in trajectory tracking and swing angle suppression despite the presence of parameter variations and external disturbances as in the case of offshore cranes.

1 Introduction

The massive increase in shipping demand as well as the prospect of having more larger mega container ships result immense pressure to ports to handle the surge in cargos. However, many ports face that expanding outwards is not a feasible option to reduce the pressures due to land constraints. As a result, they are examining alternative ways to cope with the potential surge in cargo handling demands. One possible option is to improve the efficiency and productivity so that they not only can handle the surge in cargos but also allow reduction in operational cost to take place, which would enable the ports to stay competitive [Yin *et al.*, 2011]. One of the ways to improve port efficiency is open-sea loading/unloading of containers [Ngo and Hong, 2012]. In doing so, a relatively small ship called the mobile harbour equipped with a crane loads/unloads containers from a large anchored container ship called the mother ship. Figure 1 shows the typical arrangement of a mother ship and a mobile harbour. As a result, port congestion due to the increased of cargo ships traffic can be minimized.

From the crane control literature, various control methods have been proposed for trajectory tracking and sway suppression of gantry cranes [Abdel-Rahman *et al.*, 2003]. These methods include open-loop control, such as input shaping [Blackburn *et al.*, 2010]; and closed-loop control, such as linear [Omar and Nayfeh, 2005], adaptive [Yang and Yang, 2007], fuzzy logic [Chang and Chiang, 2008], and nonlinear controls [Almutairi and Zribi, 2009; Bartolini *et al.*, 2002; Fang *et al.*, 2003]. Research on cranes' control and automation has focused on addressing challenges in their offshore operations [Skaare and Egeland, 2006; Messineo and Serrani, 2009; Küchler *et al.*, 2011; Raja Ismail *et al.*, 2012]. Ngo and Hong [2012] introduced the model of offshore gantry crane and its control strategy. However, obtaining a quick response of load transfer remains a challenge due to a heavier of container mass as compared to conventional cranes payload. Besides, the control method proposed in the study has considered the rope hoist length as a constant.

Sliding mode control offers a good capability to deal with uncertainties and nonlinearities of a plant. The methodology is based on keeping exactly a properly chosen dynamic constraint by means of high-frequency control switching, and is known as robust and very accurate. Unfortunately, its general application may be restricted, i.e., for an output sliding function to be zeroed, the standard sliding mode may keep the sliding function equal to zero only if the outputs relative degree is one [Levant, 2007]. High-frequency control switching may also cause the undesired chattering effect [Boiko *et al.*, 2010]. Higher-order sliding modes remove the relative-degree restriction and, if properly designed, can practically eliminate the chattering.

This paper presents a second-order sliding mode control for an offshore container crane. At first, the offshore crane is modeled as the extension of the proposed model

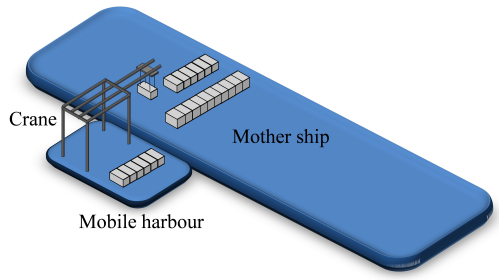

Figure 1: Arrangement of mother ship and mobile harbour.

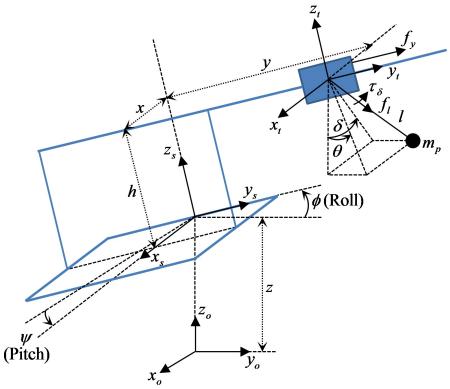

Figure 2: Motion of the crane on the mobile harbour.

by Ngo and Hong [2012] by considering the rope length as a variable due to load hoisting. Then a second-order sliding mode controller is synthesized to control the gantry crane which is located on a mobile harbour. The controller is designed so that the crane trolley position and hoisting rope length can track their respective reference trajectories while the longitudinal and lateral sway angles are suppressed. A stability analysis and simulations are performed to prove the asymptotic stability of the closed-loop system.

2 System Modelling

The offshore crane system considered in this study is a crane vessel (mobile harbour) which loads/unloads containers from a large container ship (mother ship) [Ngo and Hong, 2012] as shown in Figure 1. The coordinates system of the offshore crane is shown in Figure 2 where (x_0, y_0, z_0), (x_s, y_s, z_s), and (x_t, y_t, z_t) are respectively represent the coordinate frames of the mother ship, the mobile harbour, and the trolley. m_t and m_p are respectively the masses of the trolley and the payload, x and y represent the position of the gantry and the trolley, h is the crane height, l is the rope length, and θ and δ are respectively the longitudinal and the lateral sway angles of the load. The control forces f_y and f_l apply respectively at the trolley and hoist. Since f_y can only control the longitudinal sway, a control torque τ_δ is applied to the rope to control the lateral sway. Variables z, ϕ, and ψ are respectively the heave, roll, and yaw of the mobile harbour. By using the Langrangian formulation, he dynamic model of the offshore crane system can be cast in the form of

$$\mathbf{M}(\mathbf{q})\ddot{\mathbf{q}} + \mathbf{W}_0(\mathbf{q}, \dot{\mathbf{q}}) = \boldsymbol{\tau}_0, \tag{1}$$

where $\mathbf{M}(\mathbf{q})$ is the inertia matrix while $\mathbf{W}_0(\mathbf{q}, \dot{\mathbf{q}})$ is the lump of centrifugal-Coriolis $\mathbf{C}(\mathbf{q}, \dot{\mathbf{q}})\dot{\mathbf{q}}$, gravity $\mathbf{G}(\mathbf{q})$, and disturbances $\mathbf{f}(\mathbf{q}, \dot{\mathbf{q}})$ components, such that $\mathbf{W}_0(\mathbf{q}, \dot{\mathbf{q}}) = \mathbf{C}(\mathbf{q}, \dot{\mathbf{q}})\dot{\mathbf{q}} + \mathbf{G}(\mathbf{q}) + \mathbf{f}(\mathbf{q}, \dot{\mathbf{q}})$. The matrices $\mathbf{M}(\mathbf{q})$, $\mathbf{W}_0(\mathbf{q}, \dot{\mathbf{q}})$ and $\boldsymbol{\tau}_0$ are respectively defined as

$$\mathbf{M}(\mathbf{q}) = \begin{bmatrix} m_{11} & m_{12} & m_{13} & m_{14} \\ m_{21} & m_{22} & 0 & 0 \\ m_{31} & 0 & m_{33} & 0 \\ m_{41} & 0 & 0 & m_{44} \end{bmatrix}$$

$$\mathbf{W}_0(\mathbf{q}, \dot{\mathbf{q}}) = \begin{bmatrix} w_1 & w_2 & w_3 & w_4 \end{bmatrix}^T$$

$$\boldsymbol{\tau}_0 = \begin{bmatrix} f_y & f_l & \tau_\delta & 0 \end{bmatrix}^T,$$

where

$$\begin{aligned}
m_{11} &= m_t + m_p \\
m_{12} &= m_{21} = m_p \left[-\sin\phi\cos\theta\cos(\delta - \psi) + \cos\phi\sin\theta \right] \\
m_{13} &= m_{31} = m_p l \sin\phi\cos\theta\sin(\delta - \psi) \\
m_{14} &= m_{41} = m_p l \left[\sin\phi\sin\theta\cos(\delta - \psi) + \cos\phi\cos\theta \right] \\
m_{22} &= m_p \\
m_{33} &= m_p l^2 \cos^2\theta \\
m_{44} &= m_p l^2,
\end{aligned}$$

and where in the case of no disturbances, i.e. $\mathbf{f}(\mathbf{q}, \dot{\mathbf{q}}) = 0$:

$$\begin{aligned}
w_1 &= (m_t + m_p) \Big[-x\ddot{\psi}\sin\phi - h\ddot{\phi} - h\dot{\psi}^2\sin\phi\cos\phi \\
&\quad + (g + \ddot{z})\cos\psi\sin\phi - \left(\dot{\psi}^2\sin^2\phi + \dot{\phi}^2 \right) y \Big] \\
&\quad + m_p \Big[2\dot{l}\dot{\delta}\sin\phi\cos\theta\sin(\delta - \psi) \\
&\quad + 2\dot{l}\dot{\theta}\sin\phi\sin\theta\cos(\delta - \psi) + 2\dot{l}\dot{\theta}\cos\phi\cos\theta \\
&\quad + l\left(\dot{\theta}^2 + \dot{\delta}^2 \right)\sin\phi\cos\theta\cos(\delta - \psi) \\
&\quad - l\dot{\theta}^2\cos\phi\sin\theta - 2l\dot{\theta}\dot{\delta}\sin\phi\sin\theta\sin(\delta - \psi) \Big] \\
w_2 &= m_p \Big[-2\dot{l}\dot{\theta}\cos\theta\sin\theta - l\left(\dot{\theta}^2 + \dot{\delta}^2 \right)\cos^2\theta \\
&\quad - 2\dot{y}\dot{\phi}\cos\phi\cos\theta\cos(\delta - \psi) - 2\dot{y}\dot{\psi}\sin\phi\cos\theta\sin(\delta - \psi) \\
&\quad - y\ddot{\psi}\sin\phi\cos\theta\sin(\delta - \psi) - y\ddot{\phi}\cos\phi\cos\theta\cos(\delta - \psi) \\
&\quad + y\left(\dot{\psi}^2 + \dot{\phi}^2 \right)\sin\phi\cos\theta\cos(\delta - \psi)
\end{aligned}$$

$$
\begin{aligned}
&- 2y\dot{\psi}\dot{\phi}\cos\phi\cos\theta\sin(\delta-\psi)\\
&- h\ddot{\psi}\cos\phi\cos\theta\sin(\delta-\psi) + h\ddot{\phi}\sin\phi\cos\theta\cos(\delta-\psi)\\
&+ h\left(\dot{\psi}^2+\dot{\phi}^2\right)\cos\phi\cos\theta\cos(\delta-\psi)\\
&+ 2h\dot{\psi}\dot{\phi}\sin\phi\cos\theta\sin(\delta-\psi) + x\ddot{\psi}\cos\theta\cos(\delta-\psi)\\
&+x\dot{\psi}^2\cos\theta\sin(\delta-\psi) - (g+\ddot{z})\cos\theta\cos\delta\Big]\\
w_3 = m_p l\Big[&-2l\dot{\delta}\dot{\theta}\sin\theta\cos\theta + 2\dot{l}\dot{\delta}\cos^2\theta\\
&+ 2\dot{y}\dot{\phi}\cos\phi\cos\theta\sin(\delta-\psi) - 2\dot{y}\dot{\psi}\sin\phi\cos\theta\cos(\delta-\psi)\\
&- y\ddot{\psi}\sin\phi\cos\theta\cos(\delta-\psi) + y\ddot{\phi}\cos\phi\cos\theta\sin(\delta-\psi)\\
&- y\left(\dot{\psi}^2+\dot{\phi}^2\right)\sin\phi\cos\theta\sin(\delta-\psi)\\
&- 2y\dot{\psi}\dot{\phi}\cos\phi\cos\theta\cos(\delta-\psi)\\
&- h\ddot{\psi}\cos\phi\cos\theta\cos(\delta-\psi) - h\ddot{\phi}\sin\phi\cos\theta\sin(\delta-\psi)\\
&- h\left(\dot{\psi}^2+\dot{\phi}^2\right)\cos\phi\cos\theta\sin(\delta-\psi)\\
&+ 2h\dot{\psi}\dot{\phi}\sin\phi\cos\theta\cos(\delta-\psi) - x\ddot{\psi}\cos\theta\sin(\delta-\psi)\\
&+x\dot{\psi}^2\cos\theta\cos(\delta-\psi) + (g+\ddot{z})\cos\theta\sin\delta\Big]\\
w_4 = m_p l\Big[&2\dot{l}\dot{\theta} + 2\dot{y}\dot{\psi}\sin\phi\sin\theta\sin(\delta-\psi)\\
&+ 2\dot{y}\dot{\phi}\cos\phi\sin\theta\cos(\delta-\psi) - 2\dot{y}\dot{\phi}\sin\phi\cos\theta\\
&+ 2y\dot{\psi}\dot{\phi}\cos\phi\sin\theta\sin(\delta-\psi) - y\dot{\phi}^2\cos\phi\cos\theta\\
&- y\left(\dot{\psi}^2+\dot{\phi}^2\right)\sin\phi\sin\theta\cos(\delta-\psi)\\
&- y\ddot{\phi}\sin\phi\cos\theta + h\dot{\phi}^2\sin\phi\cos\theta\\
&+ y\ddot{\psi}\sin\phi\sin\theta\sin(\delta-\psi) - h\ddot{\phi}\cos\phi\cos\theta\\
&+ y\ddot{\phi}\cos\phi\sin\theta\cos(\delta-\psi) - x\dot{\psi}^2\sin\theta\sin(\delta-\psi)\\
&- x\ddot{\psi}\sin\theta\cos(\delta-\psi) + l\dot{\delta}^2\sin\theta\cos\theta\\
&- 2h\dot{\psi}\dot{\phi}\sin\phi\sin\theta\sin(\delta-\psi)\\
&- h\left(\dot{\psi}^2+\dot{\phi}^2\right)\cos\phi\sin\theta\cos(\delta-\psi)\\
&+ h\ddot{\psi}\cos\phi\sin\theta\sin(\delta-\psi)\\
&-h\ddot{\phi}\sin\phi\sin\theta\cos(\delta-\psi) + (g+\ddot{z})\sin\theta\cos\delta\Big].
\end{aligned}
$$

The control torque τ_δ is produced by adjusting the tensions in the additional ropes such that

$$\tau_\delta = (d_1-d_2)f_0 + (d_1+d_2)\Delta f,$$

where f_0 is the initial tension in each additional rope, Δf is the variational force exerting at the hydraulic cylinders to adjust the tensions in the additional ropes at two sides of the trolley, i.e. $f_1 = f_0 + \Delta f$ and $f_2 = f_0 - \Delta f$ for lateral sway control, and d_1 and d_2 are the distances from the trolley centre to the additional ropes, which are defined as follows:

$$
\begin{aligned}
d_1 &= \frac{bl\cos(\psi-\delta)}{\sqrt{(b-a)^2+l^2+2l(b-a)\sin(\psi-\delta)}}\\
d_2 &= \frac{bl\cos(\psi-\delta)}{\sqrt{(b-a)^2+l^2-2l(b-a)\sin(\psi-\delta)}},
\end{aligned}
$$

in which a and b are respectively the specific distances from the spreader centre to the pulley at the spreader side and from the trolley centre to the pulley at the trolley side [Ngo and Hong, 2012]. Then (1) can be rewritten as

$$\mathbf{M}(\mathbf{q})\ddot{\mathbf{q}} + \mathbf{W}(\mathbf{q},\dot{\mathbf{q}}) = \boldsymbol{\tau}, \tag{2}$$

where

$$
\begin{aligned}
\mathbf{W}(\mathbf{q},\dot{\mathbf{q}}) &= \begin{bmatrix} w_1 & w_2 & \dfrac{w_3-(d_1-d_2)f_0}{d_1+d_2} & w_4\end{bmatrix}^T\\
\boldsymbol{\tau} &= \begin{bmatrix} f_y & f_l & \Delta f & 0\end{bmatrix}^T.
\end{aligned}
$$

3 Second-order Sliding Mode Control

This section presents the design of the control development for trajectory tracking and antisway control of the offshore crane.

3.1 The Control Algorithm

The vector of generalised coordinates can be partitioned as $\mathbf{q}^T = \begin{bmatrix}\mathbf{q}_a^T & \mathbf{q}_u^T\end{bmatrix}$ and where $\mathbf{q}_a$ and $\mathbf{q}_u$ are the actuated and unactuated state vectors respectively. Similarly we partition the control vector as $\boldsymbol{\tau}^T = \begin{bmatrix}\mathbf{u}^T & 0\end{bmatrix}$. The partitioned vectors are defined as follows:

$$\mathbf{q}_a = \begin{bmatrix} y & l & \delta\end{bmatrix}^T, \quad \mathbf{q}_u = \theta$$

$$\mathbf{u} = \begin{bmatrix} f_y & f_l & \Delta f\end{bmatrix}^T.$$

Then (2) can be rewritten as

$$\begin{bmatrix}\mathbf{M}_{aa}(\mathbf{q}) & \mathbf{M}_{au}(\mathbf{q})\\ \mathbf{M}_{ua}(\mathbf{q}) & \mathbf{M}_{uu}(\mathbf{q})\end{bmatrix}\begin{bmatrix}\ddot{\mathbf{q}}_a\\ \ddot{\mathbf{q}}_u\end{bmatrix} + \begin{bmatrix}\mathbf{W}_a(\mathbf{q},\dot{\mathbf{q}})\\ \mathbf{W}_u(\mathbf{q},\dot{\mathbf{q}})\end{bmatrix} = \begin{bmatrix}\mathbf{u}\\ 0\end{bmatrix}, \tag{3}$$

where

$$
\begin{aligned}
\mathbf{M}_{aa} &= \begin{bmatrix} m_{11} & m_{12} & m_{13}\\ m_{21} & m_{22} & 0\\ m_{31} & 0 & m_{33}\end{bmatrix}\\
\mathbf{M}_{au} = \mathbf{M}_{ua}^T &= \begin{bmatrix} m_{14} & 0 & 0\end{bmatrix}^T, \quad \mathbf{M}_{uu} = m_{44}\\
\mathbf{W}_a &= \begin{bmatrix} w_1 & w_2 & \dfrac{w_3-(d_1-d_2)f_0}{d_1+d_2}\end{bmatrix}^T, \quad \mathbf{W}_u = w_4.
\end{aligned}
$$

By substituting $\ddot{\mathbf{q}}_u = -\mathbf{M}_{uu}^{-1}(\mathbf{M}_{ua}\ddot{\mathbf{q}}_a + \mathbf{W}_u)$ obtained from the second row of (3) into the first row, we get the following form

$$\overline{\mathbf{M}}(\mathbf{q})\ddot{\mathbf{q}}_a + \overline{\mathbf{W}}(\mathbf{q},\dot{\mathbf{q}}) = \mathbf{u}, \tag{4}$$

where $\overline{\mathbf{M}} = \mathbf{M}_{aa} - \mathbf{M}_{au}\mathbf{M}_{uu}^{-1}\mathbf{M}_{ua}$ and $\overline{\mathbf{W}} = \overline{\mathbf{C}}\dot{\mathbf{q}}_a + \overline{\mathbf{G}} + \bar{\mathbf{f}} = -\mathbf{M}_{au}\mathbf{M}_{uu}^{-1}\mathbf{W}_u + \mathbf{W}_a$. Note that (4) is written such that the property $\dot{\overline{\mathbf{M}}} = \overline{\mathbf{C}} + \overline{\mathbf{C}}^T$ holds.

The tracking problem consists in finding a control action guaranteeing that $\lim_{t\to\infty} \mathbf{q}(t) = \mathbf{q}^d(t)$ where $\mathbf{q}^d(t) = \begin{bmatrix} y^d(t) & l^d(t) & 0 & 0 \end{bmatrix}^T$ represent the reference trajectories for the vectors of generalized coordinates. By defining the tracking error as $\mathbf{e} = \mathbf{q} - \mathbf{q}^d$, similarly, it can be partitioned as $\mathbf{e}^T = \begin{bmatrix} \mathbf{e}_a^T & \mathbf{e}_u^T \end{bmatrix}$, where

$$\mathbf{e}_a = \begin{bmatrix} y - y^d & l - l^d & \delta \end{bmatrix}^T, \quad \mathbf{e}_u = \theta,$$

where $\mathbf{e}_a(t)$ and $\mathbf{e}_u(t)$ are the tracking error vectors of the actuated and unactuated generalized coordinates.

Let us define the vector of sliding functions as

$$\boldsymbol{\sigma} = \begin{bmatrix} \sigma_1 \\ \sigma_2 \\ \sigma_3 \end{bmatrix} = \begin{bmatrix} \dot{y} - \dot{y}^d + \lambda_1(y - y^d) + \gamma\dot{\theta} + \lambda_4\theta \\ \dot{l} - \dot{l}^d + \lambda_2(l - l^d) \\ \dot{\delta} + \lambda_3\delta \end{bmatrix}$$

or in a more convenience form

$$\boldsymbol{\sigma} = \dot{\mathbf{q}}_a - \dot{\mathbf{q}}_a^r, \tag{5}$$

where $\dot{\mathbf{q}}_a^r$ is given by

$$\dot{\mathbf{q}}_a^r = \dot{\mathbf{q}}_a^d - \Lambda_a(\mathbf{q}_a - \mathbf{q}_a^d) - \Gamma\dot{\theta} - \Lambda_u\theta, \tag{6}$$

in which $\Lambda_a = \mathrm{diag}(\lambda_1, \lambda_2, \lambda_3)$, $\Lambda_u = \begin{bmatrix} \lambda_4 & 0 & 0 \end{bmatrix}^T$ and $\Gamma = \begin{bmatrix} \gamma & 0 & 0 \end{bmatrix}^T$. Thus, from (5) the second-order derivative of the sliding function is

$$\ddot{\boldsymbol{\sigma}} = \varphi(\mathbf{q}, \dot{\mathbf{q}}, \mathbf{u}) + \overline{\mathbf{M}}^{-1}(\mathbf{q})\dot{\mathbf{u}}, \tag{7}$$

where $\varphi(\mathbf{q}, \dot{\mathbf{q}}, \mathbf{u}) = -\overline{\mathbf{M}}^{-1}(\mathbf{q})[\dot{\overline{\mathbf{M}}}(\mathbf{q})\ddot{\mathbf{q}}_a + \dot{\overline{\mathbf{C}}}(\mathbf{q}, \dot{\mathbf{q}})\dot{\mathbf{q}}_a + \overline{\mathbf{C}}(\mathbf{q}, \dot{\mathbf{q}})\ddot{\mathbf{q}}_a + \overline{\mathbf{G}}(\mathbf{q}) + \dot{\bar{\mathbf{f}}}(\mathbf{q}, \dot{\mathbf{q}})] - \dot{\ddot{\mathbf{q}}}_a^r$. We assume that the second-order derivative of the sliding function is bounded by a known function, i.e. $|\ddot{\sigma}_i| \leq \Upsilon_i(\cdot)$ [Pisano and Usai, 2011]. In order to simplify the control synthesis, it is assumed that a constant value Υ_{M_i} can be found such that

$$|\Upsilon_i(\cdot)| \leq \Upsilon_{M_i}. \tag{8}$$

Consider an auxiliary system constituted by a double integrator with output $\mathbf{x}_1$ and input $\mathbf{v}$ defined as

$$\begin{aligned} \dot{\mathbf{x}}_1 &= \mathbf{x}_2 \\ \dot{\mathbf{x}}_2 &= \mathbf{v}. \end{aligned} \tag{9}$$

By denoting $\boldsymbol{\varepsilon}_1 = \boldsymbol{\sigma} - \mathbf{x}_1$, we obtain

$$\begin{aligned} \dot{\boldsymbol{\varepsilon}}_1 &= \boldsymbol{\varepsilon}_2 \\ \dot{\boldsymbol{\varepsilon}}_2 &= \ddot{\boldsymbol{\sigma}} - \mathbf{v}, \end{aligned} \tag{10}$$

where $\boldsymbol{\varepsilon}_1$ is assumed bounded such that $|\varepsilon_{1_i}| \leq \varepsilon_{1_{i_M}}$. The equivalent control of the system (9) can be obtained once the second-order sliding mode has been established on the manifold $\boldsymbol{\varepsilon}_1 = \boldsymbol{\varepsilon}_2 = 0$, i.e. $\mathbf{v}_{\mathrm{eq}} = \ddot{\boldsymbol{\sigma}} = \varphi(\mathbf{q}, \dot{\mathbf{q}}, \mathbf{u}) + \overline{\mathbf{M}}^{-1}(\mathbf{q})\dot{\mathbf{u}}$. This leads to the equivalent representation of system (9) as follows:

$$\begin{aligned} \dot{\mathbf{x}}_1 &= \mathbf{x}_2 \\ \dot{\mathbf{x}}_2 &= \mathbf{v}_{\mathrm{eq}} = \ddot{\boldsymbol{\sigma}} = \varphi(\mathbf{q}, \dot{\mathbf{q}}, \mathbf{u}) + \overline{\mathbf{M}}^{-1}(\mathbf{q})\dot{\mathbf{u}}. \end{aligned} \tag{11}$$

The equivalent system (11) can be stabilized by using first-order sliding mode control. Let us define the sliding function as

$$\mathbf{s} = \mathbf{x}_2 + \Lambda_x\mathbf{x}_1, \tag{12}$$

where $\Lambda_x = \mathrm{diag}(\lambda_{x1}, \lambda_{x2}, \lambda_{x3})$. The sliding function (12) can steer the system (11) onto the sliding manifold $\mathbf{s} = 0$ by defining a suitable discontinuous control $\dot{\mathbf{u}}$.

The proposed control algorithms for the control derivative $\dot{\mathbf{u}}$ and the auxiliary control signal $\mathbf{v}$ are defined as

$$\dot{u}_i = -(\Psi_{M_i} + \eta_i)\,\mathrm{sign}\, s_i \tag{13}$$

$$v_i = (2\Upsilon_{M_i} + \eta_i)\,\mathrm{sign}\left(\varepsilon_{1_i} - \frac{1}{2}\varepsilon_{1_{i_M}}\right),\ i = 1, 2, 3. \tag{14}$$

where η_i is a positive constant and the definition of constant Ψ_{M_i} will be discussed in the next subsection.

3.2 Stability of the Equivalent System

In the equivalent dynamics, the condition $\boldsymbol{\varepsilon}_1 = \boldsymbol{\varepsilon}_2 = 0$ has been already achieved, which implies

$$\begin{aligned} \mathbf{x}_1 &= \boldsymbol{\sigma} = \dot{\mathbf{q}}_a - \dot{\mathbf{q}}_a^r \\ \mathbf{x}_2 &= \dot{\boldsymbol{\sigma}} = \ddot{\mathbf{q}}_a - \ddot{\mathbf{q}}_a^r \\ \ddot{\mathbf{q}}_a &= \mathbf{s} - \Lambda_x\boldsymbol{\sigma} + \ddot{\mathbf{q}}_a^r. \end{aligned} \tag{15}$$

To prove the stability of the equivalent system by means of control algorithm (13), we choose the following Lyapunov function candidate

$$V = \frac{1}{2}\mathbf{s}^T\overline{\mathbf{M}}\mathbf{s}.$$

Then, the derivative of V is

$$\begin{aligned} \dot{V} &= \frac{1}{2}\left(\dot{\mathbf{s}}^T\overline{\mathbf{M}}\mathbf{s} + \mathbf{s}^T\overline{\mathbf{M}}\dot{\mathbf{s}}\right) + \frac{1}{2}\mathbf{s}^T\dot{\overline{\mathbf{M}}}\mathbf{s} \\ &= \mathbf{s}^T\overline{\mathbf{M}}\dot{\mathbf{s}} + \frac{1}{2}\mathbf{s}^T\dot{\overline{\mathbf{M}}}\mathbf{s} \end{aligned}$$

since $\overline{\mathbf{M}}$ is symmetric. From (12), (11) and (5),

$$\dot{\mathbf{s}} = \dot{\mathbf{x}}_2 + \Lambda_x\mathbf{x}_2 = \ddot{\boldsymbol{\sigma}} + \Lambda_x\mathbf{x}_2 = \ddot{\mathbf{q}}_a - \dot{\ddot{\mathbf{q}}}_a^r + \Lambda_x\mathbf{x}_2. \tag{16}$$

Thus, we have

$$\dot{V} = \mathbf{s}^T\left(\overline{\mathbf{M}}\ddot{\mathbf{q}}_a - \overline{\mathbf{M}}\dot{\ddot{\mathbf{q}}}_a^r + \overline{\mathbf{M}}\Lambda_x\mathbf{x}_2\right) + \frac{1}{2}\mathbf{s}^T\dot{\overline{\mathbf{M}}}\mathbf{s}.$$

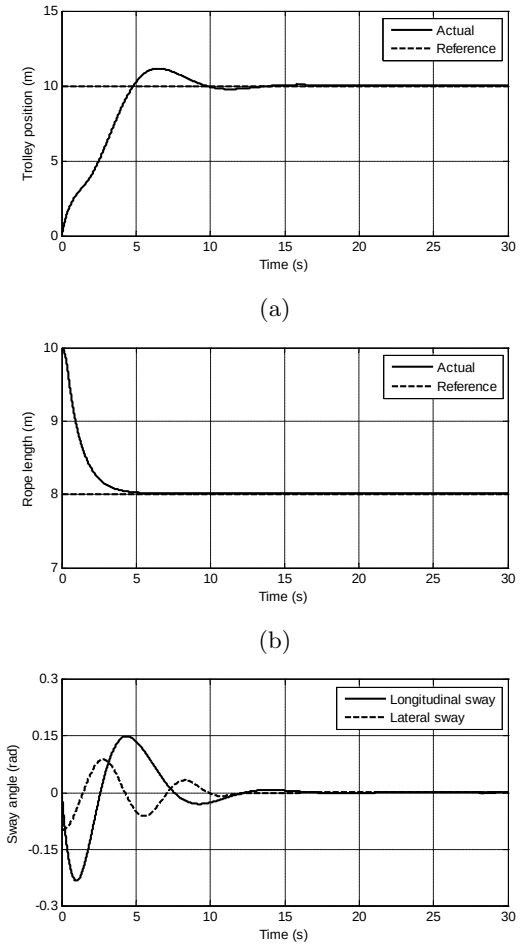

Figure 3: (a) Trolley position; (b) rope length; and (c) swing angles; when the mobile harbour is stationary, i.e. $\phi = 0$ and $\psi = 0$.

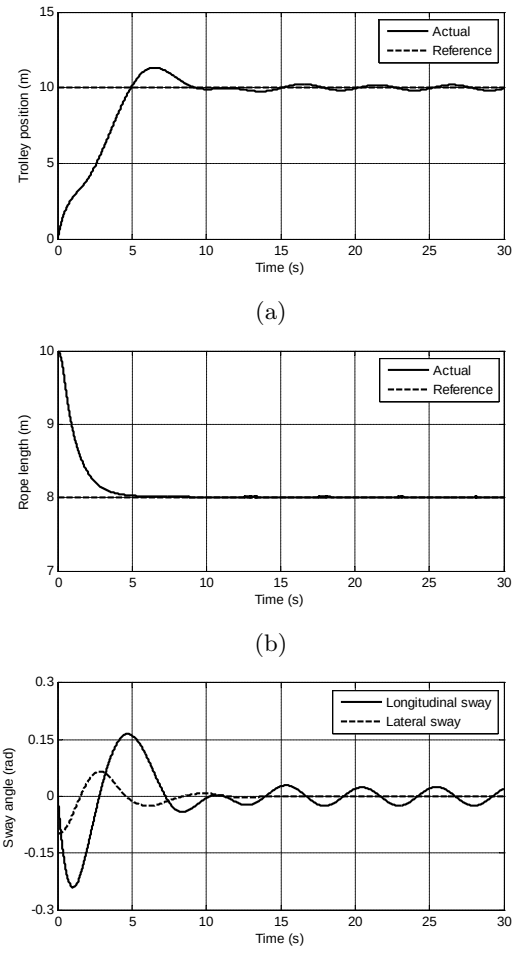

Figure 4: (a) Trolley position; (b) rope length; and (c) swing angles; when $\phi = 0.02 \sin 1.25t$ rad and $\psi = 0.01 \sin 1.25t$ rad.

By differentiating (4), it can be shown that $\overline{\mathbf{M}}\dot{\ddot{\mathbf{q}}}_a = -\dot{\overline{\mathbf{M}}}\ddot{\mathbf{q}}_a - \overline{\mathbf{C}}\ddot{\mathbf{q}}_a - \dot{\overline{\mathbf{C}}}\dot{\mathbf{q}}_a - \dot{\overline{\mathbf{G}}} - \dot{\bar{\mathbf{f}}} + \dot{\mathbf{u}}$. Hence, from this equation and the last equation of (15), the derivative of the Lyapunov function becomes

$$\begin{aligned}\dot{V} &= \mathbf{s}^T \Big[-\dot{\overline{\mathbf{M}}}\ddot{\mathbf{q}}_a - \overline{\mathbf{C}}\ddot{\mathbf{q}}_a - \dot{\overline{\mathbf{C}}}\dot{\mathbf{q}}_a - \dot{\overline{\mathbf{G}}} - \dot{\bar{\mathbf{f}}} \\ &\qquad -\overline{\mathbf{M}}\dot{\ddot{\mathbf{q}}}_a^r + \overline{\mathbf{M}}\Lambda_x \mathbf{x}_2 + \dot{\mathbf{u}} \Big] + \frac{1}{2}\mathbf{s}^T \dot{\overline{\mathbf{M}}}\mathbf{s} \\ &= \mathbf{s}^T \Big[-\dot{\overline{\mathbf{M}}} \left(\mathbf{s} - \Lambda_x \boldsymbol{\sigma} + \ddot{\mathbf{q}}_a^r \right) - \overline{\mathbf{C}} \left(-\Lambda_x \boldsymbol{\sigma} + \ddot{\mathbf{q}}_a^r \right) \\ &\qquad -\dot{\overline{\mathbf{C}}}\dot{\mathbf{q}}_a - \dot{\overline{\mathbf{G}}} - \dot{\bar{\mathbf{f}}} - \overline{\mathbf{M}}\dot{\ddot{\mathbf{q}}}_a^r + \overline{\mathbf{M}}\Lambda_x \mathbf{x}_2 + \dot{\mathbf{u}} \Big] \\ &\quad + \frac{1}{2}\mathbf{s}^T \left(\dot{\overline{\mathbf{M}}} - 2\overline{\mathbf{C}} \right) \mathbf{s} \\ &= \mathbf{s}^T \left[\Psi(\mathbf{q}, \dot{\mathbf{q}}, \mathbf{u}, \mathbf{q}_a^r, \dot{\mathbf{q}}_a^r, \ddot{\mathbf{q}}_a^r, \dot{\ddot{\mathbf{q}}}_a^r) + \dot{\mathbf{u}} \right]\end{aligned}$$

since the matrix $\dot{\overline{\mathbf{M}}} - 2\overline{\mathbf{C}}$ is skew-symmetric while all terms that do not contain the derivative of control signal $\dot{\mathbf{u}}$ are lumped into the function $\Psi(\cdot)$. We also assume that this function is bounded, i.e. $|\Psi_i(\cdot)| \leq \Psi_{M_i}$. Therefore, by substituting (13) into the last equation, it can be shown that

$$\dot{V} \leq -\eta_i \mathbf{s}^T \mathbf{s},$$

which implies that the surface $\mathbf{s} = 0$ is globally reached in a finite time.

4 Results and Discussion

In this study the values of the crane parameters are listed as $m_t = 6000$ kg, $m_p = 20000$ kg, $h = 10$ m, $x = 5$ m, $a = 0.5$ m, $b = 4$ m, $f_0 = 8000$ N, and $g = 9.8065$ m-s^{-2}. The mobile harbour motion (z, ϕ, ψ) are considered as disturbance, where $z = 0.02 \sin 1.25t$ m while ϕ and

ψ will be defined based on the scenarios studied. The controller parameters used in the simulations are $\lambda_1 = 10$, $\lambda_2 = \lambda_3 = 1$, $\lambda_4 = -1$, $\gamma = 0.1$, $\lambda_{x_i} = 1$, $\Psi_{M_i} = 50 \times 10^3$, $\Upsilon_{M_i} = 10 \times 10^3$, $\eta_i = 30$ and $\varepsilon_{1_{i_M}} = 10$, $\forall i = 1, 2, 3$. The initial value of the generalized coordinates vector is chosen as $(y_0, l_0, \delta_0, \theta_0) = (0\,\text{m}, 10\,\text{m}, -0.1\,\text{rad}, 0\,\text{rad})$.

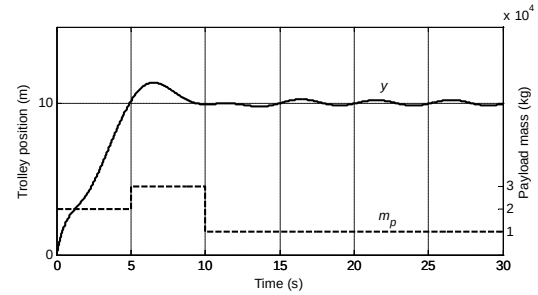

(a)

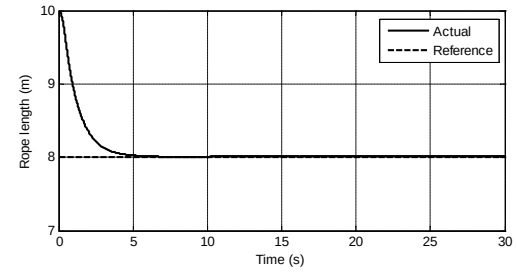

(b)

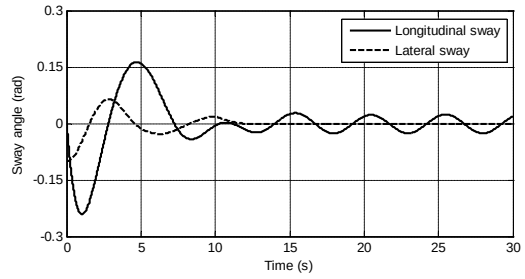

(c)

Figure 5: (a) Trolley position and payload mass; (b) rope length; and (c) swing angles; when $\phi = 0.02 \sin 1.25t$ rad, $\psi = 0.01 \sin 1.25t$ rad, and payload mass is varied.

Several scenarios were considered for simulation to assess the capability of the proposed controller. The first one is by considering that the mobile harbour is stationary, i.e. both its roll and pitch angles are set to zero ($\phi = 0$ and $\psi = 0$) as shown in Figure 3. In this case, both longitudinal and lateral swing angles are totally suppressed a few seconds after the trolley reached its reference position. The second scenario considered in the study is with the presence of both roll and pitch angles such that $\phi = 0.02 \sin 1.25t$ rad and $\psi = 0.01 \sin 1.25t$ rad. In practical, this situation can occur due to the presence of ocean wave movements. As shown in Figure 4, the lateral sway is suppressed to zero but the longitudinal sway keep swinging with amplitude 0.03 rad. This is due to the longitudinal sway is controlled indirectly by the control force f_y which is applied to the trolley.

To demonstrate the robustness of the controller, the payload is varied between 10×10^3 to 30×10^3 kg. From Figure 5, it is shown that the trolley position trajectory and swing angles unperturbed by the presence of payload variation, which is similar with Figure 4. However, the rope length trajectory is slightly affected by the payload variation with 0.02 m steady state error.

In all three scenarios, the proposed second-order sliding mode controller has provided a shorter rise time of the trolley position, which is 4.02 s, as compared to Ngo and Hong [2012], which is 8.20 s. However, this faster response comes at the cost of 10.1% overshoot.

5 Acknowledgement

This paper was supported, in part, by the New South Wales Government through its Environmental Trust under grant 2012/RDS/0034.

6 Conclusion

In this paper we have presented second-order sliding mode control schemes for the trajectory tracking and anti-swing control problem of an offshore container crane system. The extended model by considering the flexibility of the crane hoisting rope length has been discussed. A sliding surface vector, a second-order sliding mode control law, and the asymptotic stability of the closed-loop system in the Lyapunov sense have been developed. High performance in trajectory tracking and swing angle suppression are obtained either when the mobile harbour is stationary or moving with pitch and roll angles. Robust control performance is also obtained when the system is subject to external disturbances and payload variations. Simulation results are provided to indicate the effectiveness of the proposed method.

References

[Abdel-Rahman *et al.*, 2003] Eihab M. Abdel-Rahman, Ali H. Nayfeh, and Ziyad N. Masoud. Dynamics and Control of Cranes: A Review. *J. Vibration and Control*, 9(7):863–908, July 2003.

[Almutairi and Zribi, 2009] Naif B. Almutairi and Mohamed Zribi. Sliding mode control of a three-dimensional overhead crane. *J. Vibration and Control*, 15(11):1679–1730, November 2009.

[Bartolini *et al.*, 2002] Giorgio Bartolini, Alessandro Pisano, and Elio Usai. Second-order sliding-mode control of container cranes. *Automatica*, 38(10):1783–1790, October 2002.

[Blackburn *et al.*, 2010] David Blackburn, William Singhose, J. Kitchen, Vlad Patrangenaru, Jason Lawrence, Tatsuaki Kamoi, and Ayako Taura. Command shaping for nonlinear crane dynamics. *J. Vibration and Control*, 16(4):477–501, April 2010.

[Boiko *et al.*, 2010] I. Boiko, L. Fridman, and M. I. Castellanos. Analysis of Second-Order Sliding-Mode Algorithms in the Frequency Domain. *IEEE Trans. Automatic Control*, 49(6):946–950, June 2004.

[Chang and Chiang, 2008] Cheng-Yuan Chang and Kuo-Hung Chiang. Fuzzy projection control law and its application to the overhead crane. *Mechatronics*, 18(10):607–615, December 2008.

[Fang *et al.*, 2003] Y. Fang, W. E. Dixon, D. M. Dawson, and E. Zergeroglu. Nonlinear coupling control laws for an underactuated overhead crane system. *IEEE/ASME Trans. Mechatronics*, 8(3):418-423, September 2003.

[Küchler *et al.*, 2011] Sebastian Küchler, Tobias Mahl, Jörg Neupert, Klaus Schneider, and Oliver Sawodny. Active control for an offshore crane using prediction of the vessels motion. *IEEE/ASME Trans. Mechatronics*, 16(2):297-309, April 2011.

[Levant, 2007] Arie Levant. Principles of 2-sliding mode design. *Automatica*, 43(4):576–586, April 2007.

[Messineo and Serrani, 2009] Saverio Messineo and Andrea Serrani. Offshore crane control based on adaptive external models. *Automatica*, 45(11):2546–2556, November 2009.

[Ngo and Hong, 2012] Quang Hieu Ngo and Keum-Shik Hong. Sliding-mode antisway control of an offshore container crane. *IEEE/ASME Trans. Mechatronics*, 17(2):201–209, April 2012.

[Omar and Nayfeh, 2005] Hanafy M. Omar and Ali H. Nayfeh. Gantry cranes gain scheduling feedback control with friction compensation. *J. Sound and Vibration*, 281(1-2):1–20, March 2005.

[Pisano and Usai, 2011] A. Pisano and E. Usai. Sliding mode control: A survey with applications in math. *J. Mathematics and Computers in Simulation*, 81(5):954–979, January 2011.

[Raja Ismail *et al.*, 2012] R.M.T. Raja Ismail, Nguyen D. That, and Quang P. Ha. Observer-based trajectory tracking for a class of underactuated Lagrangian systems using higher-order sliding modes. In *Proc. IEEE International Conference on Automation Science and Engineering*, pages 1200–1205, Seoul, Korea, August 2012. IEEE Robotics and Automation Society.

[Skaare and Egeland, 2006] Bjørn Skaare and Olav Egeland. Parallel force/position crane control in marine operations. *IEEE J. Oceanic Engineering*, 31(3):143–152, July 2006.

[Yang and Yang, 2007] Jung Hua Yang and Kuang Shine Yang. Adaptive coupling control for overhead crane systems. *Mechatronics*, 17(2-3):143–152, March–April 2007.

[Yin *et al.*, 2011] Xiao Feng Yin, Li Pheng Khoo, and Chun-Hsien Chen. A distributed agent system for port planning and scheduling. *J. Advanced Engineering Informatics*, 25(3):403-412, August 2011.